FOLIA MEDICA CRACOVIENSIA
Vol. LVI, 3, 2016: 11–19
PL ISSN 0015-5616

3D visualization of the intratemporal course of the facial canal using computed micro-tomography

Magdalena Kozerska[1], Janusz Skrzat[1], Alexandru Spulber[1], Sebastian Wroński[2], Jacek Tarasiuk[2]

[1]Department of Anatomy, Jagiellonian University Medical College
ul. Kopernika 12, 31-034 Kraków, Poland
[2]AGH University of Science and Technology
Faculty of Physics and Applied Computer Science
al. Mickiewicza 30, 30-065 Kraków, Poland

Corresponding author: Dr hab. Janusz Skrzat, Department of Anatomy
Jagiellonian University Medical College
ul. Kopernika 12, 31-034 Kraków, Poland
Phone/Fax: +48 12 422 95 11; E-mail: jskrzat@poczta.onet.pl

Abstract: The current study presents high resolution reconstructions showing the course of the facial canal within the temporal bone and visualizes the spatial orientation of the subsequent segments of the facial canal. 3D reconstructions of the facial canal were created from micro-CT data obtained from the right and left human temporal bones of an adult individual of the male sex. For this purpose, volume and surface rendering was applied. 3D models of the facial canal and adjacent osseous structures comprehensively revealed its intricate course and depicted the spatial orientation of its subsequent segments: labyrinthine, tympanic and mastoid. The labyrinthine segment of the facial canal was clearly displayed in the horizontal plane whereas the tympanic and mastoid segments were entirely visible in the sagittal plane, which lines up along the long axis of the petrous part of the temporal bone.

Key words: facial canal, petrous bone, computed micro-tomography.

Introduction

The facial canal, also known as the Fallopian canal, was first described by Gabriel Fallopius in the 16th-century. It contains the seventh cranial nerve, termed the facial nerve, and blood vessels such as the stylomastoid artery and superficial petrosal artery. The facial canal runs through the temporal bone from the fundus of the internal acoustic meatus to the stylomastoid foramen and its course resembles the letter 'Z'. Its length is approximately 30 mm, which makes the facial canal the longest osseous canal in the human skull [1–3].

The facial canal is divided into three segments: the labyrinthine, the tympanic and the mastoid segment, and moreover has two turns named as the first genu and second genu of the facial canal. The first segment of the facial canal (labyrinthine) is the shortest when compared to the remaining segments. The labyrinthine segment emerges from the fundus of the internal acoustic meatus and ends in the geniculate ganglion fossa. Here, the facial canal bends, forming the first genu. The labyrinthine segment is also the narrowest of all parts of the facial canal. Its size reaches 3–5 mm [3, 4].

The tympanic segment constitutes the second segment of the facial canal. It extends horizontally from the first genu to the second genu of the facial canal (to the pyramidal eminence). The tympanic segment descends obliquely along the medial wall of the tympanic cavity, forming the prominence of the facial canal. This segment lies below the lateral semicircular canal and above the oval window and cochleariform process. The length of the tympanic segment can reach up to 10 mm [2, 5, 6].

The third segment of the facial canal (mastoid) is the longest of all parts of the canal and measures over 12 mm. The mastoid segment descends from the second genu vertically and slightly laterally towards the stylomastoid foramen via which it exits the temporal bone. Out of all facial canal segments, the mastoid segment is the most variable in length. This feature is related to the size of the mastoid process (particularly its length), which depends on the age and sex of the individual [3, 4, 7].

The facial canal is a structure of interest in otosurgery because it serves as a significant anatomical landmark during surgical operations inside the middle ear. However, the relatively small size and tortuous course of the facial canal make it difficult to image by the standard computed tomography used in clinical examination. Especially, identification of the tympanic segment in standard CT-scans can be problematic due to its relatively thin bony wall or the presence of potential dehiscences [2, 3].

Thereby, the aim of this study was to present high resolution reconstructions showing the course of the facial canal within the temporal bone and visualize spatial orientation of its subsequent segments: labyrinthine, tympanic and mastoid.

Material and methods

Three-dimensional visualization of the facial canal topography was performed on two samples of the temporal bone (right and left) dissected from the skull of an adult individual of the male sex. Selected samples did not reveal any signs of damage or pathology. The temporal bones used in the current study belong to the osteological collection housed in the Department of Anatomy, Medical College of the Jagiellonian University (Kraków, Poland).

The method of 3D reconstruction of the facial canal was based on serial micro-CT scans of the petrous parts of the temporal bones, obtained from a Nanotom 180N device produced by GE Sensing & Inspection Technologies Phoenix X-ray Gmbh. For detailed imaging of the internal anatomy of the petrous bone the following parameters were set for the X-ray tube: V = 70 kV and I = 250 μA. The reconstructions of the scanned samples were performed with the aid of the GE software datos|x ver. 2.1.0 using the Feldkamp algorithm for cone beam X-ray CT [8]. The tomograms were registered on a Hamamatsu 2300 × 2300 pixel detector. The final voxel size used in volumetric reconstructions was 18 μm. The post-reconstruction data were denoised, cropped and converted to 8-bit images using the VGStudio Max 2.1 software (http://www.volumegraphics.com/en/products/vgstudio-max/). Further, volume rendering of the facial canal and neighboring structures of the middle and inner ear was performed by the CTVox software. 3D volume reconstructions were adjusted for optimal display of the facial canal viewed in different projections. The best visual effects of the rendered anatomical structures were attained by altering parameters of the transfer function which controlled the style and range of displayed voxels in the 3D volume reconstructions.

To obtain 3D mesh models of the facial canal, we used polygon meshes which represented the surface of the facial canal and adjacent structures as a set of connected triangles. For this purpose we used CTAn software which created 3D mesh models of the petrous part of the temporal bone from the serial micro-CT scans. Further, 3D mesh models were processed with MeshLab software to improve its quality. With the aid of Meshmixer software, we sectioned off the region containing the facial canal from adjacent osseous structures. In this way we eliminated parts of the model (unwanted anatomical structures) which obscured or covered up the facial canal.

The course of the facial canal was projected to reference planes positioned according to selected segments of the facial canal. The labyrinthine segment of the facial canal was oriented in the horizontal plane, whereas the tympanic and mastoid segments were in the sagittal plane which passes along the long axis of the petrous bone. This part of the study was performed in the CTVox and Meshmixer softwares. Both the CTVox and CTAn softwares are supplied by the SkyScan company (http://bruker-microct.com/products/downloads.htm). The MeshLab software is available from http://meshlab.sourceforge.net and the Meshmixer software from http://www.meshmixer.com.

Results

Completed 3D reconstructions showed the close-up morphological appearance and topography of the facial canal (Fig. 1). It is clearly visible that the facial canal is approximately orientated in two planes: horizontal and sagittal. However, when we analyzed position of the subsequent segments of the facial canal we perceived that their orientation in 3D space is more complex. To better show the course of the facial canal, the lateral and tegmental walls of the tympanic cavity were cut away in 3D reconstructions. Such reconstructions clarified how the facial canal traverses the petrous part of the temporal bone and reveals its relationship to the tympanic cavity and other osseous structures of the ear (Fig. 1A). From these reconstructions, it is easily noticeable that the original part of the facial canal — the labyrinthine segment — runs horizontally to the first genu from which the facial canal turns sharply backward.

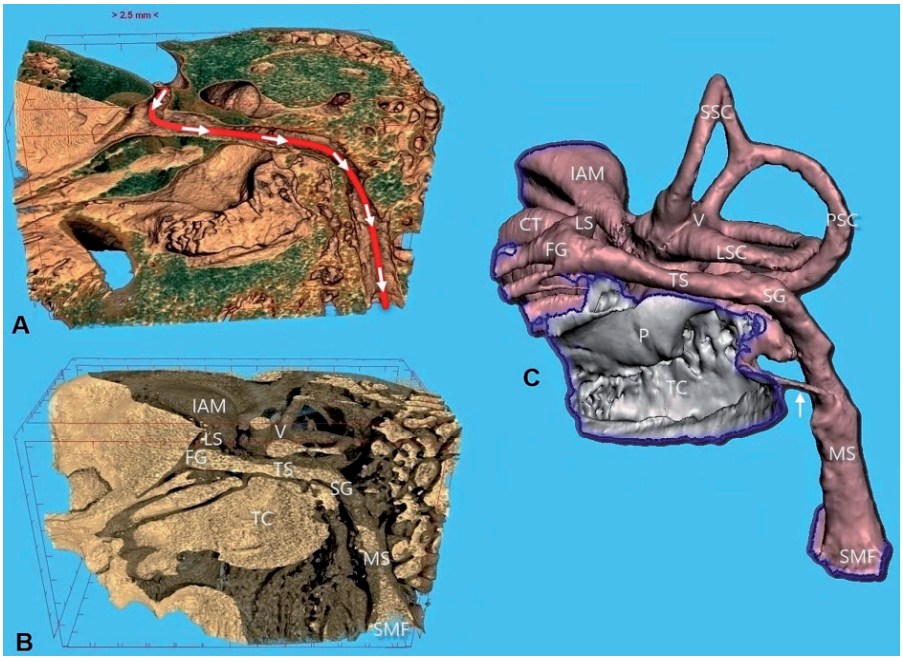

Fig. 1. Intratemporal course of the left facial canal and its topography visualized from micro-CT data using volume and surface rendering techniques. A — The course of the facial canal is indicated by the arrows, opacity of the bone tissue around the facial canal is preserved; B — the bone surrounded the facial canal is rendered transparent; C — corresponding 3D mesh model of the facial canal showing its relationship to the tympanic cavity and the labyrinth viewed in lateral aspect. Segments of the facial canal were marked as: LS — labyrinthine segment, TS — tympanic segment, MS — mastoid segment, FG — first genu, SG — second genu, IAM — internal acoustic meatus, SSC — superior semicircular canal, LSC — lateral semicircular canal, PSC — posterior semicircular canal, CT — cochlear turn, V — vestibule, TC — tympanic cavity, P — promontory, SMF — stylomastoid foramen. The canal for the chorda tympani is marked by the arrow.

Further, the facial canal (the tympanic segment) runs obliquely within the medial wall of the tympanic cavity to the second genu, where it changes its course and becomes the mastoid segment, descending vertically down toward the stylomastoid foramen located in the cranial base.

The 3D reconstructions (volume and surface rendering images) clearly presented the relationship of each segment of the facial canal to the surrounding osseous ear components: the tympanic cavity, cochlea, and the semicircular canals (Fig. 1B, Fig. 1C). However, spatial relationships between anatomical structures were much better emphasized in 3D mesh models than in volume renderings because parts of the bone matrix surrounding the facial canal and the osseous labyrinth could be removed by virtual dissection of the 3D mesh model. This exposed the course of the facial canal in relation to the tympanic cavity and the osseous labyrinth. The 3D mesh models also exposed the course of the canal for the chorda tympani which emerges from the mastoid segment of the facial canal and leads to the tympanic cavity (Fig. 1C).

Both volume rendering and surface rendering of the facial canal revealed that its morphological appearance varies along its course. We observed that the labyrinthine segment was narrow at the beginning and bulged gradually towards the first genu. The tympanic segment was locally flattened, particularly in the middle part. The mastoid

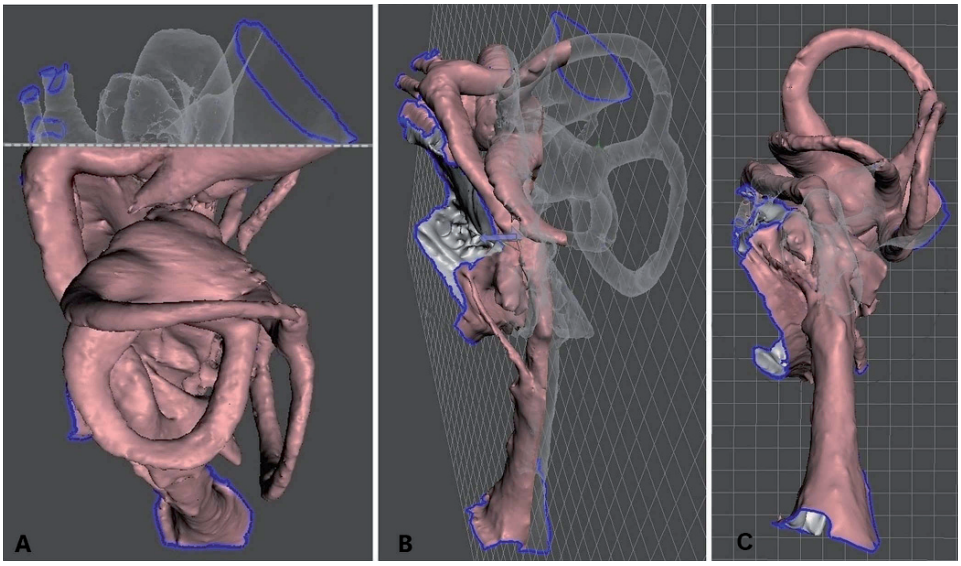

Fig. 2. 3D mesh models showing the positions of the subsequent segments of the facial canal according to the reference planes; anatomical structures depicted as transparent are located behind the reference plane. A — the reference plane (dashed line) passes frontally to the labyrinthine segment; superior view, B — the reference plane (lattice) passes through the facial canal origin (the fundus of the internal acoustic meatus) and its outlet from the temporal bone (the stylomastoid foramen); supero-posterior view, C — the reference plane (lattice) is orientated frontally to the mastoid segment; posterior view.

segment was approximately tubular in shape and its distal part was considerably widened. These morphological features are well visible in Fig. 1C which presents the surface of the facial canal combined into a 3D mesh model and in Fig. 1B which presents a volume rendering whose transfer function was designed for displaying the air that fills the lumen of the facial canal, making the impression for creating the endocast of the canal.

Three-dimensional imaging of the facial canal obtained by volume and surface rendering of the micro-CT data revealed the whole spectrum of the morphological varieties present within the shape and course of the facial canal.

Discussion

Imaging of the facial nerve and its canal is typically performed by using both clinical computed tomography (CT) and magnetic resonance (MR) for evaluation of known or suspected pathology in this area of the skull, and for performing morphometric analysis of facial canal anatomy [3, 4, 9–11]. Despite the fact that high quality images can be obtained by using high resolution clinical computed tomography, the facial canal can only be visualized partially on standard CT-scans. This seems to be insufficient for detailed visualization of the entire course of the facial canal. Nevertheless, Fatterpekar *et al.* managed to present the entire course of the facial canal in 3-D volume rendered CT images, whose quality is comparable to reconstructions obtained from micro-CT data [12].

Up until now, only a few papers presented the morphology and topography of the facial canal in a 3-dimensional way using micro-CT data [13, 14]. Shin *et al.* showed not only 3-D reconstruction images of the facial canal using volume rendering, but also determined various dimensions of this canal in adult individuals (ranged 23–96 years) [14]. Skadorwa *et al.* applied the same imaging technique (computed microtomography) for depicting the facial canal in fetal temporal bones (aged 16–27 Hbd). However, in their paper, the facial canal is not presented in a 3-D manner but in single micro-CT scans which only present selected parts of the facial canal in the sagittal and horizontal sections. Obtained single sections allowed accurate measurements of the fetal facial canal [15].

In the literature, the trajectory of the facial canal is defined as having the shape of the letter 'Z' [3, 6, 16]. It should be noted that such statements concerning the Z-shaped course of the facial canal should be treated as a simplification of its real course, whose perception depends on the visualization mode and orientation of the reconstructed volume.

According to Tüccar *et al.* it is possible to demonstrate the entire Z-shaped course of the facial canal using special CT sections [16]. Virapongse *et al.* also stated that certain section planes are recommended for better visualization of the facial canal

segments [17]. The frontal and horizontal planes are recommended for best imaging the labyrinthine segment and first genu of the facial canal. The tympanic segment, the second genu, and the mastoid segment are best visible in the sagittal plane [17, 18]. Our observations of the facial canal course reconstructed from micro-CT data confirms the abovementioned statements. The findings regarding the bilateral course of the facial canal were illustrated in Fig. 3.

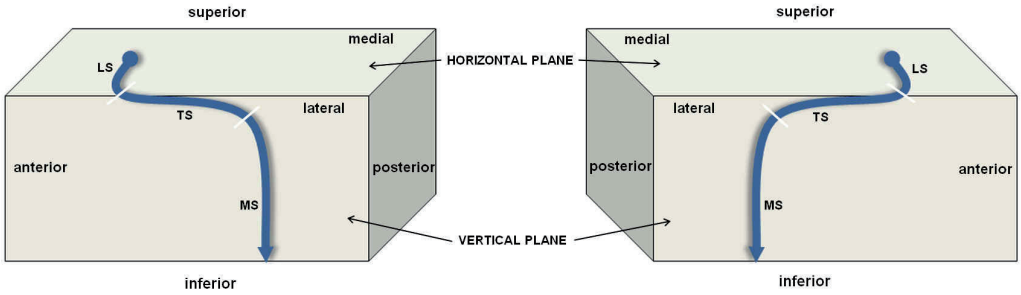

Fig. 3. A diagram showing directions of the facial canal course and positions of its subsequent segments to the horizontal and vertical (sagittal) planes observed in the left and right temporal bones. LS — labyrinthine segment, TS — tympanic segment, MS — mastoid segment. Positions of the first and second genu are marked by short white lines which also demarcate the borders between the segments of the facial canal.

In our study, the created models of the facial canal showed its morphological form which varies along its course. This refers mainly to the local narrowing and flattening of the facial canal which occurs in the labyrinthine and tympanic segments [14, 19, 20]. The 3D models of the facial canal introduced in our study appeared very beneficial for visualizing these morphological features (Fig. 1, Fig. 2). It should also be noticed that single CT-sections are insufficient for overall presentation of the facial canal trajectory, because the canal declines locally from a cutting plane. Therefore the facial canal can be observed on multiple CT scans viewed separately or composed into a stack. In clinical evaluation this is a preferable imaging technique for diagnosing facial canal malformations [10, 16].

Volume rendering of the facial canal performed in our study allowed the illustration of anatomical details which cannot be captured by clinical tomography or are only weakly visible in CT-scans. Therefore, data obtained from computed micro-tomography can enrich contemporary knowledge on the variation of facial canal morphology and topography.

The 3D models created in our study allowed precise evaluation of the trajectory and the shape of the facial canal, as well as its relation to the neighboring osseous structures. These models turn out to be more useful for demonstrating facial canal topography than volume rendering images. Hence, they can be used in comparative

studies aimed at analyzing facial canal geometry performed on more numerous samples.

Conclusions

Volume reconstructions as well as 3D mesh models obtained from micro-CT data are efficient for visualizing the shape and topography of the facial canal. An appropriate adjustment of the clipping planes allows tracing of the path of the facial canal as it passes through the petrous bone and depiction of the positions of each segment (the labyrinthine, the tympanic and the mastoid) relative to the other structures of the middle and inner ear. The 3D mesh models and reference planes expose the positions of the subsequent segments of the facial canal much better than volume rendering reconstructions.

Acknowledgements

The study was conducted with approval (KBET/198/B/2014) of the Bioethics Committee of the Jagiellonian University. The authors declare that they have no conflicts of interest concerning this article.

References

1. *Macchi V., Porzionato A., Morra A., De Caro R.*: Gabriel Falloppius (1523–1562) and the facial canal. Clin Anat. 2014; 27 (1): 4–9. PMID: 23553994.
2. *Mansour S., Magnan J., Haidar H., Nicolas K., Louryan S.*: Comprehensive and clinical anatomy of the Middle Ear. Springer-Verlag Berlin/Heidelberg. 2013; 1–159. doi 10.1007/978-3-642-36967-4.
3. *Weiglein A.H., Anderhuber W., Jakse R., Einspieler R.*: Imaging of the facial canal by means of multiplanar angulated 2-D-high-resolution CT-reconstruction. Surg Radiol Anat. 1994; 16 (4): 423–427. PMID: 7725200.
4. *Phillips C.D., Bubash L.A.*: The facial nerve: anatomy and common pathology. Semin Ultrasound CT MR. 2002; 23 (3): 202–217. PMID: 12168997.
5. *Chandra S., Goyal M., Gandhi D., Gera S., Berry M.*: Anatomy of the facial nerve in the temporal bone : HRCT. Indian J Radiol Imaging. 1999; 9 (1): 5–8.
6. *Mortazavi M.M., Latif B., Verma K., Adeeb N., Deep A., Griessenauer C.J., Tubbs R.S., Fukushima T.*: The fallopian canal: a comprehensive review and proposal of a new classification. Childs Nerv Syst. 2014; 30 (3): 387–395. PMID: 24322603.
7. *Fujita S., Nakashima S., Sando I., Takahashi H.*: Postnatal developmental changes in facial nerve morphology. Computer-aided 3-D reconstruction and measurement. Eur Arch Otorhinolaryngol. 1994; 251 (7): 434–438. PMID: 7857633.
8. *Feldkamp L.A., Davis L.C., Kress J.W.:* Practical cone-beam algorithm. J Opt Soc Am. 1984; 1 (6): 612–619. doi: 10.1364/JOSAA.1.000612.
9. *Kollias S.S., Valavanis A., Linder T., Fisch U.*: High resolution T2-weighted magnetic resonance imaging of the facial nerve. New Horizons in Facial Nerve Research and Facial Expression. 1998; 151–157. Kugler publications, Hague/Netherlands.

10. *Valavanis A., Kubik S., Oguz M.*: Exploration of the facial nerve canal by high-resolution computed tomography: anatomy and pathology. Neuroradiology. 1983; 24 (3): 139–147. PMID: 6298657.
11. *Yu Z., Wang Z., Yang B., Han D., Zhang L.*: The value of preoperative CT scan of tympanic facial nerve canal in tympanomastoid surgery. Acta Otolaryngol. 2011; 131 (7): 774–778. PMID: 21453222.
12. *Fatterpekar G.M., Doshi A.H., Dugar M., Delman B.N., Naidich T.P., Som P.M.*: Role of 3D CT in the evaluation of the temporal bone. Radiographics. 2006; 26 (1): 117–132. PMID: 17050510.
13. *Lane J.I., Witte R.J.*: Temporal Bone. An Imaging Atlas. Springer-Verlag Berlin/Heidelberg. 2010; 1–109. doi: 10.1007/978-3-642-02210-4.
14. *Shin K.J., Gil Y.C., Lee J.Y., Kim J.N., Song W.C., Koh K.S.*: Three-Dimensional Study of the Facial Canal Using Microcomputed Tomography for Improved Anatomical Comprehension. Anat Rec. 2014; 297 (10): 1808–1816. PMID: 24990524.
15. *Skadorwa T., Maślanka M., Ciszek B.*: The morphology and morphometry of the fetal fallopian canal: a microtomographic study. Surg Radiol Anat. 2015; 37 (6): 677–684. PMID: 25480106.
16. *Tüccar E., Tekdemir I., Aslan A., Elhan A., Deda H.*: Radiological anatomy of the intratemporal course of facial nerve. Clin Anat. 2000; 13 (2): 83–87. PMID: 10679852.
17. *Virapongse C., Rothman S.L., Kier E.L., Sarwar M.*: Computed tomographic anatomy of the temporal bone. AJR Am J Roentgenol. 1982; 139 (4): 739–749. PMID: 6981936.
18. *Cooper M.H., Archer C.R., Kveton J.F.*: Correlation of high-resolution computed tomography and gross anatomic sections of the temporal bone: Part I. The facial nerve. Am J Otol. 1987; 8 (5): 375–384. PMID: 3688197.
19. *Nakashima S., Sando I., Takahashi H., Fujita S.*: Computer-aided 3-D reconstruction and measurement of the facial canal and facial nerve. I. Cross-sectional area and diameter: preliminary report. Laryngoscope. 1993; 103 (10): 1150–1156. PMID: 8412453.
20. *Vianna M., Adams M., Schachern P., Lazarini P.R., Paparella M.M., Cureoglu S.*: Differences in the diameter of facial nerve and facial canal in bell's palsy — a 3-dimensional temporal bone study. Otol Neurotol. 2014; 35 (3): 514–518. PMID: 24518410.